Bioorganic Chemistry 92 (2019) 103183

Contents lists available at ScienceDirect

Bioorganic Chemistry

journal homepage: www.elsevier.com/locate/bioorg

New A_{2A} adenosine receptor antagonists: a structure-based upside-down interaction in the receptor cavity

Catia Lambertucci[a,1], Andrea Spinaci[a,1], Michela Buccioni[a], Diego Dal Ben[a], Michael Alliance Ngouadjeu Ngnintedem[a], Sonja Kachler[b], Gabriella Marucci[a], Karl-Norbert Klotz[b], Rosaria Volpini[a,*]

[a] School of Pharmacy, Medicinal Chemistry Unit, University of Camerino, Camerino, Italy
[b] Universität Würzburg, Institut für Pharmakologie und Toxikologie, Versbacher Str. 9, D-97078 Würzburg, Germany

ARTICLE INFO

Keywords:
Adenosine receptors
Purinergic receptors
Adenosine receptor ligands
Adenosine receptor antagonists
Rational design
Medicinal chemistry, molecular modeling
Radioligand binding studies

ABSTRACT

Adenosine receptor antagonists are generally based on heterocyclic core structures presenting substituents of various volumes and chemical-physical profiles. Adenine and purine-based adenosine receptor antagonists have been reported in literature. In this work we combined various substituents in the 2, 6, and 8-positions of 9-ethylpurine to depict a structure-affinity relationship analysis at the human adenosine receptors. Compounds were rationally designed trough molecular modeling analysis and then synthesized and evaluated at radioligand binding studies at human adenosine receptors. The new compounds showed affinity for the human adenosine receptors, with some derivatives endowed with low nanomolar K_i data, in particular at the A_{2A}AR subtype. The purine core proves to be a versatile core structure for the development of novel adenosine receptor antagonists with nanomolar affinity for these membrane proteins.

1. Introduction

Extracellular adenosine (Ado) plays a number of physiological roles through the stimulation of G Protein-Coupled Receptors called adenosine receptors (ARs) and known as four subtypes: A_1, A_{2A}, A_{2B}, and A_3 ARs [1,2]. Each subtype has unique pharmacological profile due to endogenous ligand affinity, intracellular effector coupling, and synthetic ligands specificity. In fact, A_1 and A_{2A} ARs are endowed with nanomolar affinity for Ado, while A_{2B} and A_3 ARs need micromolar concentrations (i.e. due to tissue damage) of the endogenous ligand to be activated. Furthermore, while the activation of A_{2A} and A_{2B} ARs takes to an increase of intracellular levels of cAMP due to stimulation of adenylyl cyclase (AC) activity, the stimulation of A_1 and A_3 ARs takes to reduction of intracellular cAMP and stimulation of phospholipase C (PLC) activity [1,2]. Each AR subtype presents different levels of expression in various tissues. Through the modulation of the activity of the different ARs, extracellular Ado regulates vascular smooth muscle tone and blood flow [3,4], heart rate and contractility [5], inflammation [6–8], sleep [9,10], and cognitive mechanisms [11]. Within the CNS, Ado modulates also neuronal plasticity and development, neuronal excitability and arousal, release of neurotransmitters, and neuroinflammation [12–16]. All together, these factors make the ARs potential (if not promising) therapeutic targets for a number of conditions including cardiovascular, inflammatory, and neurodegenerative diseases [17–21]. Besides Ado itself, therapeutically used as injectable antiarrhythmic agent, natural or synthetic AR ligands are available on the market as agonists (i.e. the coronary vasodilator Regadenoson [22]) and antagonists (the CNS stimulator caffeine [23], the bronchodilator theophylline [24], the anti-Parkinson tool istradefylline [25]). The prototypical AR antagonists are xanthines and methylxanthines, whose modifications led to derivatives endowed with potency and AR subtype selectivity [26]. Among these compounds are the above cited caffeine, theophylline, and istradefylline. A number of classes of non-xanthine derivatives have also been developed as potent and selective AR antagonists [27–30].

In the last years we developed 9-alkyladenine derivatives substituted in the 2, N^6, and 8-positions. These compounds presented different degrees of affinity and selectivity for the various AR subtypes [31–37]. More in detail, the 8-bromo-9-ethyladenine showed good affinity and moderate selectivity for the A_{2A}AR (**I**; K_i A_{2A} = 52 nM, Fig. 1); substitution of the bromine atom with a 2-furyl ring enhanced both the A_{2A} affinity and selectivity, especially *versus* the A_3 receptor

* Corresponding author at: School of Pharmacy, University of Camerino, via S. Agostino, 1, 62032 Camerino, MC, Italy.
E-mail address: rosaria.volpini@unicam.it (R. Volpini).
[1] C. Lambertucci and A. Spinaci equally contributed to the work.

https://doi.org/10.1016/j.bioorg.2019.103183
Received 2 May 2019; Received in revised form 16 July 2019; Accepted 1 August 2019
Available online 05 August 2019
0045-2068/ © 2019 Elsevier Inc. All rights reserved.

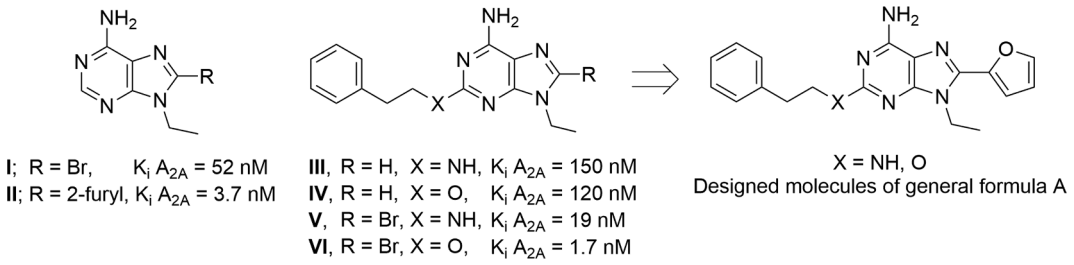

Fig. 1. Known and designed compounds of general formula A.

subtype (**II**; K_i A_{2A} = 3.7 nM). On the other hand, even the presence of a phenylethylamino or a phenylethyloxy chain in the 2-position of 9-ethyladenine favoured the interaction with the A_{2A}AR subtype leading to compound **III** and **IV**, which are endowed with a similar selectivity profile (see details within the Biological activity section). The combination of a phenylethylamino or a phenylethyloxy group in the 2-position and a bromine atom in the 8-position led to compounds endowed with enhanced A_{2A}AR affinity (**V**; K_i = 19 nM and **VI**; K_i = 1.7 nM, Fig. 1) [33,38].

Since the replacement of the 8-substituent of the 8-bromo-9-ethyladenine with a 2-furyl ring led to an improvement of the A_{2A}AR affinity [39], we hence synthesized (and here we present) 9-ethyladenine derivatives bearing a 2-furyl ring in the 8-position and a phenylethylamino or a phenylethyloxy group in the 2-position (designed molecules of general formula A, Fig. 1). On the other hand, the displacement of the phenylethylamino or the phenylethyloxy chain of **V** and **VI** from the 2- to the 6-position led to a significative decrease of the A_{2A}AR affinity (compounds **VII**: K_i = 280 nM and **VIII**: K_i = 19,300 nM, Fig. 2) [31]. For compounds **VII** and **VIII**, modeling studies suggested a particular binding mode in which the 6-substituents mimicked the role of the analogue 2-substituents of **V** and **VI**, while the 8- and 9-substituents were located almost in the same position (Fig. 2). This resulted in a sort of upside-down binding mode respect to the "canonical" binding orientation observed i.e. for the reference A_{2A} receptor ligand ZM241385. In this binding mode, however, the 6-substituted derivatives lacked the H-bond donor function corresponding to the free amine function of the 2-substituted derivatives [40]. On these bases, we designed and developed 9-ethyladenines bearing a phenylethylamino or a phenylethyloxy chain in the 6-position, a bromine atom in the 8-position, and an amine function in the 2-position (designed molecules of general formula B, Fig. 2). The presence of the amino group in the 2-position is aimed at restoring the H-bond donor function suggested by molecular modeling studies previously reported [40] and according to the "pharmacophore" hypothesis showed in Fig. 2. The new compound bearing the phenylethylamino chain in the 6-position and an 8-bromo substituent was further modified by replacing the bromine atom with a 2-furyl ring.

Finally, we also designed and synthesized 9-ethyladenines bearing various groups in the 8-position and the phenylethylamino substituent in both the 2- and 6-positions to test the effect of the combined presence of the two arylalkyl groups on the AR affinity (designed molecules of general formula C, Fig. 3). All the compounds were tested by radioligand binding studies at the human recombinant A_1, A_{2A} and A_3 ARs and the results were analysed with molecular docking studies.

2. Results and discussion

2.1. Chemistry

The synthesis of the 9-ethyl-8-(2-furyl)-2-phenylethylamine-adenine (**1**) and its 2-alkoxy analogue **2** was carried out by Suzuki coupling reaction conditions on the 8-bromo-9-ethyl-2-substituted adenine

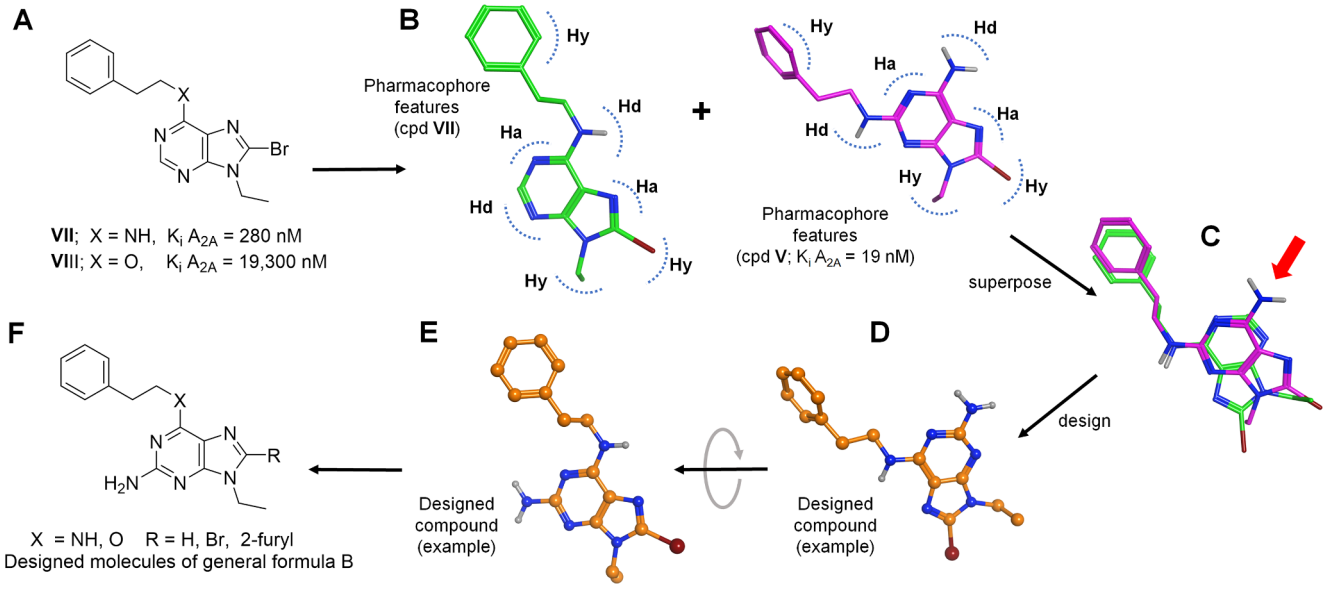

Fig. 2. Design of N^6,8-disubstituted 2-amino-9-ethyladenines. A. Previously reported N^6,8-disubstituted 9-ethyladenines [31]. B. Comparison of compounds in panel A (compound **VII** as example) with 2,8-disubstituted 9-ethyladenines (compound **V** as example) and definition of respective pharmacophore features, where Ha, Hd, and Hy are H-bond acceptor, H-bond donor and Hydrophobic pharmacophoric features, respectively. C. Superimposition of compounds **VII** and **V** with matching of pharmacophore features; compound **V** presents and additional H-bond donor group indicated by the arrow. D. Design of N^6-phenylalkyl substituted 2-amino-9-ethyladenine derivatives; the 2-amino group is inserted to restore the H-bond donor feature suggested in panel; example of designed compound; E. The same example compound, rotated view. F. Designed N^6,8-disubstituted 2-amino-9-ethyladenines to be synthesized and tested in this work.

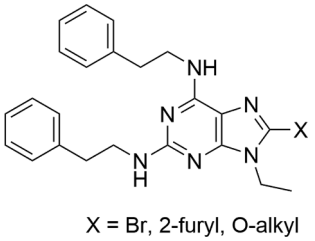

Fig. 3. Designed compounds of general formula C.

derivatives **V** and **VI**, previously prepared in our laboratory [33].

The two compounds were in turn treated with 2-(tributylstannyl) furan and bis triphenylphosphine palladium dichloride in tetrahydrofuran as solvent at 60 °C for 5 h in anhydrous conditions (Scheme 1). The synthesis of purine derivatives **7–10** was carried out starting from commercially available 2-amino-6-chloropurine (**3**; Scheme 2). Compound **3** was reacted with ethyl iodide in dry dimethylformamide (DMF), using potassium carbonate as base, under anhydrous conditions at room temperature (r.t.) as reported before [31].

After chromatography of the reaction mixture, **4** and **4a** were obtained as pure products with 66% and 21% yield, respectively. These compounds were obtained previously [31] and the structures were confirmed by UV spectra and NMR chemical shifts. In this work, for a deeper characterization, the alkylation site of the two isomers was assigned by ^{1}H-NOE difference spectroscopy in DMSO of the N^6-methyl analogues **5** and **6**, obtained by reacting **4** and **4a** with methylamine (Scheme 2). The choice to use the N^6-methyl derivatives **5** and **6** for the alkylation site assignment was due to the fact that in the case of the N7-isomer the NOE effect easily takes place when in the N^6-position there is a small group (i.e. a methyl group) that makes the H-N(6) less exchangeable. In fact, irradiation of the CH_2 protons of **5** (at 3.95 ppm) yielded a NOE at the H-C(8) and H_3-C(CH_2) protons while there was no effect on the H-N(6) proton in the resulting spectra. On the contrary, irradiation of CH_2 protons of **6** (at 4.26 ppm) yielded a NOE at the H-C(8), H_3-C(CH_2) and also at the H-N(6) protons in the resulting spectra. These data allowed an unambiguous identification of **5** as the 9-isomer and **6** as the 7-isomer (Fig. 4).

Hence, **4** was treated with phenylethylamine or phenylethyl alcohol in order to substitute the 6-chlorine atom and to obtain compounds **7** and **8**, respectively (Scheme 2). The reactions were performed using the reagents as solvents at r.t. In the case of reaction with phenylethyl alcohol, sodium hydroxide was added to catalyse the reaction.

The 6-substituted 2-amino-9-ethylpurine derivatives **7** and **8** were obtained with a yield of 78% and 57%, respectively. Reaction of these latter compounds with *N*-bromosuccinimide (NBS) in DMF, at r.t., furnished the desired 8-bromo derivatives **9** and **10** with 80 and 35% yield, respectively (Scheme 2).

To obtain the 8-furyl derivative **13,** a different synthetic pathway was set up, which allows to synthesise 2-amino-9-ethyl-8-(2-furyl) purine derivatives substituted in the 6-position with various chains. In fact, compound **4** was brominated to obtain the polyfunctionalized intermediate **11** (Scheme 3). The 8-bromo-6-cloroadenine derivative **11** was then reacted with 2-(tributylstannyl)furan in the presence of bis (triphenylphosphine)palladium (II) dichloride in DMF using Stille coupling reaction conditions.

The selective substitution of the 8-bromine atom was obtained using 2-(tributylstannyl)furan in a 1:1 equivalent ratio with the purine derivative **11**; the 8-furyl analogue **12** was obtained with a 54% yield. Replacement of the 6-chlorine atom of **12** with phenylethylamine, at r.t., furnished the desired tetrasubstituted adenine derivative **13** in 90% yield. This approach could be very useful to obtain in good yield further 6-substituted derivatives of compound **12**. Compounds **17–20** were obtained by 3 synthetic steps starting from 2,6-dichloro-9-ethylpurine (**14**, Scheme 4) obtained with the earlier reported procedure [38]. **14** Was treated with 2-phenylethylamine at 120 °C for 16 h to get the desired 9-ethyl-2-phenylethylamine-6-phenylethyladenine (**15**), with 90% yield, which was then treated with bromine and sodium acetate in acetic acid and left to react at r.t. for 12 h.

The 8-bromoderivative **16** was obtained with 85% yield as pure compound. The substitution of the 8-bromine atom with a 2-furyl group was obtained as previously described for compounds **1** and **2** (Scheme 1), to get the 9-ethyl-8-(2-furyl)-2-phenylethylamino-2-phenylethyladenine (**17**) with 29% yield. Finally, reaction of **16** with methanol or ethanol, used as solvent, or phenethyl alcohol (using tetrahydrofurane as solvent) in the presence of sodium hydroxide, furnished the 8-alkyloxy purine derivatives **18–20** (Scheme 4). These compounds were obtained by reaction at 70 °C or reflux for 17–72 h, with yield ranging from 37 to 80%.

2.2. Biological activity and molecular modeling studies

The novel adenine derivatives (**1**, **2**, **7–10**, **13**, **15–20**) were tested by evaluating their affinity at the human A_1, A_{2A} and A_3 ARs stably expressed in Chinese hamster ovary (CHO) cells. Previously published derivatives **V-VIII** were reported as reference compounds. A set of derivatives was also selected and tested at the $hA_{2B}AR$ subtype by measuring their inhibitory effects on NECA-stimulated cAMP levels in $hA_{2B}AR$ CHO cells. The results are presented in Table 1. Molecular docking analyses were performed to simulate the binding mode of the synthesized compounds at the $hA_{2A}AR$ cavity. As molecular target, we chose the high-resolution crystal structure of the $hA_{2A}AR$ in complex with the antagonist ZM241385 (http://www.rcsb.org; pdb code: 5NM4; 1.7-Å resolution [41]). Gold software [42] was employed to perform docking analyses to depict the potential binding mode of the compounds at the $hA_{2A}AR$ binding cavity. For a subset of compounds, the binding modes at a homology model of the hA_3AR [43] were also simulated with the same tools and protocols.

As already reported in the introduction part (Fig. 1), the presence of a bromine atom in the 8-position of 9-ethyl-2-phenylethylamino or 9-ethyl-2-phenylethyloxyadenine enhanced both the $A_{2A}AR$ affinity and selectivity (**III**; Ki $A_{2A}AR$ = 150 nM, select. A_1/A_{2A} = 2, A_3/A_{2A} = 21 *vs* **V**; Ki $A_{2A}AR$ = 19 nM, select. A_1/A_{2A} = 8, A_3/A_{2A} = 163; and **IV**; Ki $A_{2A}AR$ = 120 nM, select. A_1/A_{2A} = 1, A_3/A_{2A} = 60 *vs* **VI**; Ki $A_{2A}AR$ = 1.7 nM, select. A_1/A_{2A} = 13, A_3/A_{2A} = 640) [33]. Replacement of the 8-bromine atom of **V** and **VI** with a 2-furyl ring led to

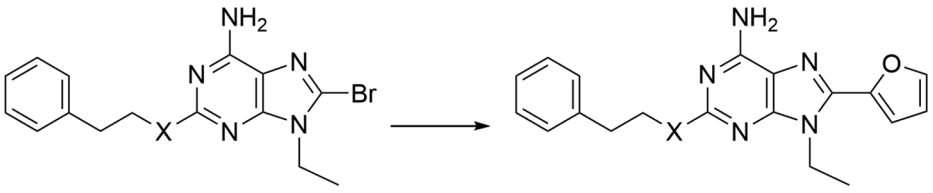

V; X = NH
VI; X = O

1; X = NH
2; X = O

Scheme 1. *Reagents and conditions:* *n*But_3Sn-(2-furyl), $(Ph_3P)_2PdCl_2$, THF, 60 °C, 5 h.

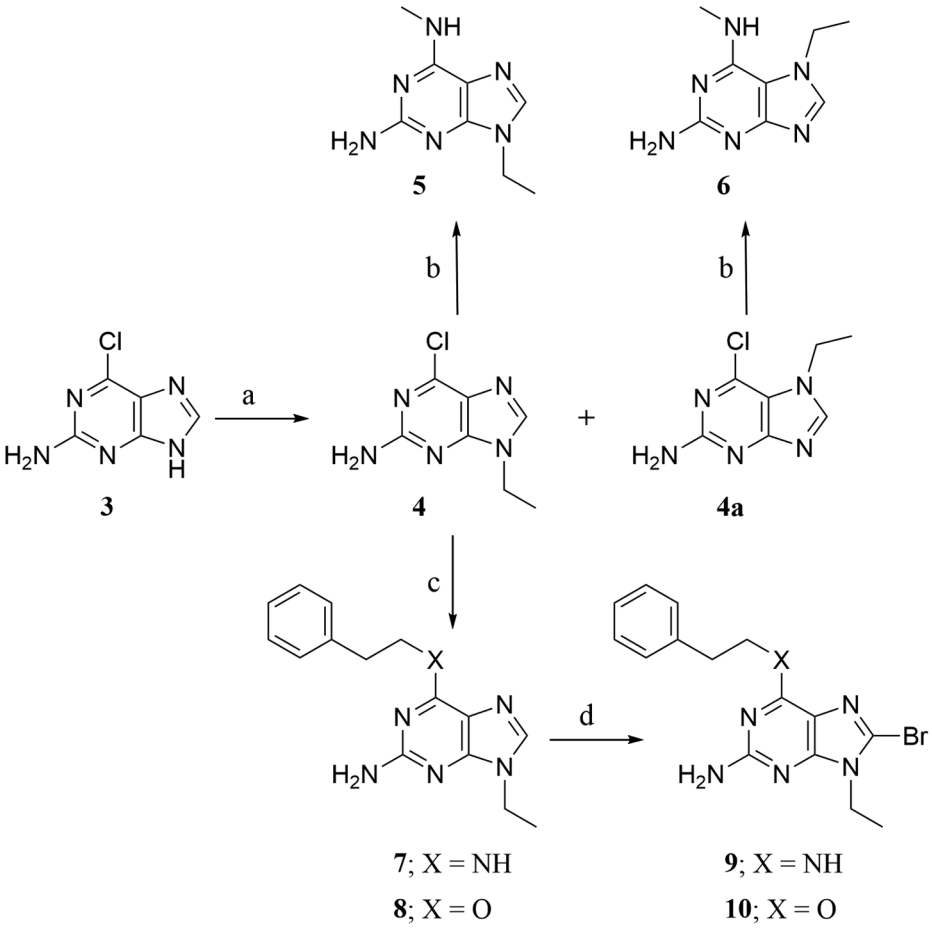

Scheme 2. *Reagents and conditions:* (a) Et-I, K_2CO_3, DMF, r.t., 5 h; (b) Me-NH_2, r.t., 16 h; (c) 1. $Ph(CH_2)_2NH_2$, r.t., 3.5 h; or 2. $Ph(CH_2)_2OH$, NaOH, r.t., 3.5 h; (d) NBS, DMF, r.t., 10–70 min.

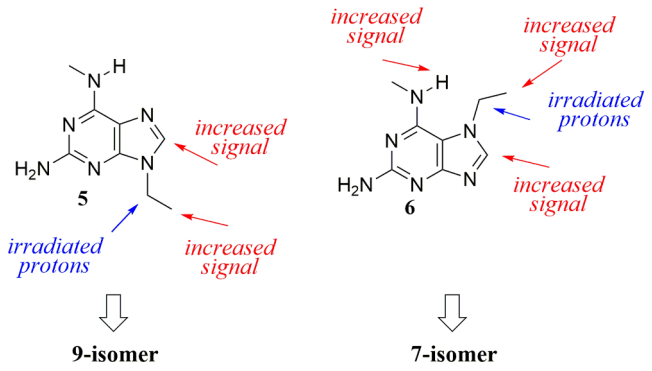

Fig. 4. Assignment of the alkylation site on compounds **5** and **6** by [^{1}H]-NMR NOE experiment. In the figure are illustrated the irradiated protons in blue and the protons giving an increased signal in red. Only in the case of compound **6**, an increased signal of the CH_3 and also at the H-N(6) was obtained upon irradiation of the CH_2 protons. This demonstrated that the CH_2 is close to the N^6-position, hence the alkylation site is the 7-position. (For interpretation of the references to colour in this figure legend, the reader is referred to the web version of this article.)

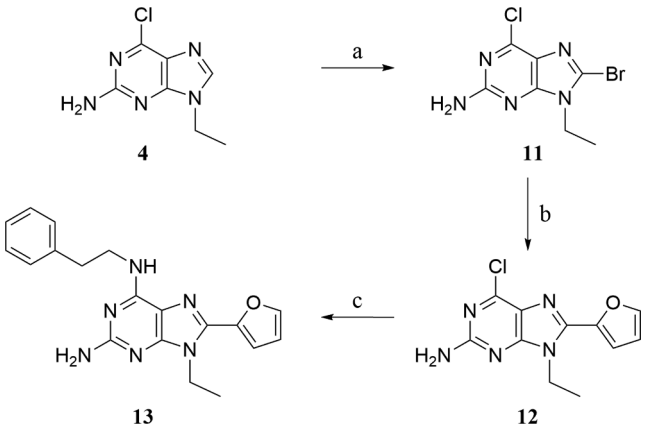

Scheme 3. *Reagents and conditions:* (a) NBS, DMF, r.t., 8 h; (b) *n*But_3Sn-(2-furyl), $(PPh_3)_2PdCl_2$, THF, 60 °C, 3 h; (c) $Ph(CH_2)_2NH_2$, r.t., 4 h.

compounds with generally enhanced affinity at ARs, but decreased selectivity for the A_{2A}AR subtype. In particular, the 9-ethyl-8-furyl-2-phenylethylaminoadenine (**1**: Ki A_{2A}AR = 3.8 nM, select. A_1/A_{2A} = 2, A_1/A_3 = 5) displayed a five-fold increased affinity respect to its 8-bromo analogue **V**, while the 9-ethyl-8-furyl-2-phenylethyloxyadenine (**2**: Ki A_{2A}AR = 2.2 nM, select. A_1/A_{2A} = 3, A_1/A_3 = 7) maintained the same A_{2A}AR affinity of **VI**.

The results of biological evaluation of compounds **7–10** (Table 1) showed that the combination of a phenylalkylamino or phenylalkyloxy group in the 6-position with a 2-amine function generally takes to compounds endowed with micromolar or high nanomolar affinity for the human ARs, with a low selectivity in some cases for the A_{2A}AR subtype.

As expected, the introduction of an 8-bromo substituent improves the affinity at all the AR subtypes with respect to the corresponding 8-unsubstituted derivatives. Among these molecules, compound **9** showed the best A_{2A}AR affinity and selectivity (**9**, Table 1; K_i A_{2A}AR = 266 nM;

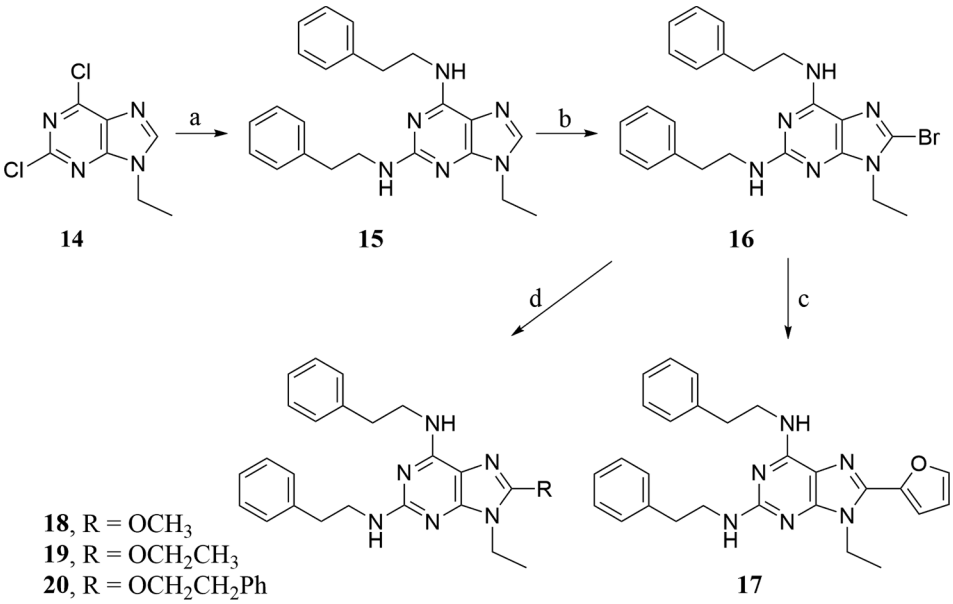

Scheme 4. *Reagents and conditions:* (a) $Ph(CH_2)_2NH_2$, 120 °C, 16 h; (b) Br_2, CH_3COONa, CH_3COOH, r.t., 12 h; (c) *n*But_3Sn-(2-furyl), $(PPh_3)_2PdCl_2$, THF, reflux, 2.5 h; (d) CH_3OH, CH_3CH_2OH or $Ph(CH_2)_2OH$/THF, NaOH, reflux, 17–72 h.

A_1/A_{2A} = 7; A_3/A_{2A} = 4). Based on the observation that compound **1** and **2**, bearing a 2-furyl group in the 8-position, showed an improved A_{2A}AR affinity with respect to the corresponding 8-bromo substituted analogues **V** and **VI**, we analogously modified compound **9** to obtain the derivative **13**. This compound showed a remarkable improvement of affinity for the ARs with respect to the corresponding 8-bromo substituted analogue **9** and resulted the compound endowed with the highest A_{2A}AR affinity (**13**, Table 2; K_i A_{2A}AR = 12 nM) among the newly 6-substituted 2-amino synthesized compounds. Among these derivatives, compounds **9** and **13** showed activity as A_{2B}AR inhibitors, even if only at micromolar level.

Results of docking studies performed at the human A_{2A}AR crystal structure showed that the 2-amino derivatives **7–10**, **13** may interact with the receptor by adopting two kinds of conformations (Fig. 5). The first one (binding mode 1, Fig. 5A) presents the purine core oriented similarly to the co-crystallized A_{2A}AR antagonist ZM241385 and similarly also to other adenine-based A_{2A}AR antagonists previously developed and reported. In detail, the bicyclic core is inserted between

Table 1
Biological activity data of the synthesized compounds at the human ARs.

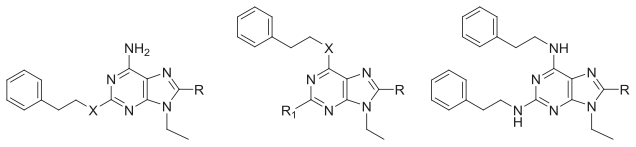

V, VI, 1, 2 VII, VIII, 7-10, 13 15-20

CPD	X	R	R_1	hA_1AR (K_i nM)[a]	$hA_{2A}AR$ (K_i nM)[b]	$hA_{2B}AR$ (IC_{50} nM)[c]	hA_3AR (K_i nM)[d]
V	NH	Br		150	19	690 *(250–1,900)*	*3,100*
VI	O	Br		23	1.7	569 *(440–734)*	*1,090*
1	NH	2-furyl		9.4 *(7.0–13)*	3.8 *(3.4–4.2)*	2,340 *(1,340–4,110)*	18 *(17–18)*
2	O	2-furyl		5.8 *(4.0–8.4)*	2.2 *(2.1–2.3)*	521 *(467–580)*	16 *(11–22)*
VII	NH	Br	H	1,540	280	2,210 *(1,460–3,350)*	2,440
VIII	O	Br	H	11,700	19,300	> 100,000	60,900
7	NH	H	NH_2	6,404 *(6,321–6,482)*	4,635 *(4,581–4,720)*	nd	> 40,000
8	O	H	NH_2	5,959 *(3,570 –8,348)*	5,044 *(2,861–7,227)*	nd	3,404 *(3,032–3,775)*
9	NH	Br	NH_2	1,931 *(1,855–2,008)*	266 *(251–296)*	5,895 *(5,735–6,108)*	1,192 *(1,104–1,265)*
10	O	Br	NH_2	2,671 *(2,535–2,730)*	1,080 *(998–1,160)*	> 30,000	1,115 *(1,035–1,198)*
13	NH	2-furyl	NH_2	96 *(70–121)*	12 *(7.3–16)*	4,000 *(3,816–4,230)*	20 *(14–27)*
15		H		440 *(401–486)*	593 *(545–630)*	> 30,000	13 *(9.3–18)*
16		Br		602 *(463–740)*	251 *(188–314)*	nd	481 *(376–586)*
17		2-furyl		293 *(226–360)*	104 *(78–130)*	> 30,000	45 *(35–55)*
18		OCH_3		798 *(595–941)*	217 *(171–263)*	nd	585 *(452–717)*
19		OCH_2CH_3		546 *(423–669)*	250 *(197–303)*	> 30,000	183 *(145–220)*
20		$O(CH_2)_2C_6H_5$		> 30,000	> 30,000	nd	1,062 *(823–1,301)*

[a] Displacement of specific [^{3}H]-CCPA binding at human A_1AR expressed in CHO cells, (n = 3–6).
[b] Displacement of specific [^{3}H]-NECA binding at human A_{2A}AR expressed in CHO cells.
[c] IC_{50} values of the inhibition of NECA-stimulated adenylyl cyclase activity in CHO cells expressing human A_{2B}AR (nd = not determined).
[d] Displacement of specific [^{3}H]-HEMADO binding at human A_3AR expressed in CHO cells. Data are expressed as geometric means, with 95% confidence limits.

Table 2
Inhibitory effect of a set of selected compounds on the NECA-induced cAMP production in CHO cells. Data are expressed as IC_{50} values (the respective K_i values at the $A_{2A}AR$ are indicated).

CPD	$hA_{2A}AR$ (K_i nM)	$hA_{2A}R$ (IC_{50} nM)
V	19	411 *(398–424)*
VI	1.7	108 *(50–166)*
1	3.8	171 *(135–207)*
7	4,635	> 50,000
8	5,044	> 50,000
9	266	5,753 *(4,776–6,730)*
10	1,080	> 50,000
13	12	962 *(696–1,228)*

residues of transmembrane (TM) domains 3, 6, and 7, making polar and hydrophobic interactions with the receptor residues.

The 8- and 9-substituents point toward the depth of the cavity while the N^6-substituent is oriented toward the extracellular environment. The alternative docking conformation (binding mode 2, Fig. 5B), presents the compound inserted in the cavity with an upside-down orientation with respect to the binding mode 1 arrangement. The 8- and 9-substituents are again pointing toward the depth of the cavity, while the 2-amino group is externally oriented. The comparison (Fig. 5A and B) and superimposition (Fig. 5C) of the two arrangements demonstrate a good agreement with the rationale presented in Fig. 2 (considering i.e. compounds **V** and **9**, or **1** and **13**). In fact, the phenylalkylamine group in the 6-position of compound **13** (binding mode 2, Fig. 5B) is located in almost the same position of the analogue group in the 2-position of **1** (Fig. 5D); analogously, the exocyclic amine groups of the same two compounds are similarly located, making analogue polar interaction with the receptor residue Asn253.

We further developed this series by introducing the phenylalkylamino group in both the 2- and 6-position, with additional 8-modifications. Results (Table 1) show that these compounds (**15–20**) are generally endowed with nanomolar affinity for the ARs, but with some selectivity for the A_3AR subtype. Compound **17** (Fig. 6), presenting a 2-furyl group in the 8-position, is endowed with a significantly improved $A_{2A}AR$ affinity (**17**, Table 1; K_i $A_{2A}AR$ = 104 nM) with respect to the 8-unsubstituted derivative **15** (**15**, Table 2; K_i $A_{2A}AR$ = 593 nM); on the other hand, compound **17** lacks selectivity for the $A_{2A}AR$ and it preferentially binds the A_3AR subtype (**17**, Table 1; K_i A_3AR = 45 nM).

Compound **15** showed a low nanomolar A_3AR affinity (**15**, Table 1; K_i A_3AR = 13 nM) with 35- and 47-fold selectivity *vs* the A_1 and A_{2A} AR subtypes, resulting the most A_3AR selective ligand of the whole group. An improved affinity for this AR subtype was not totally unexpected, as

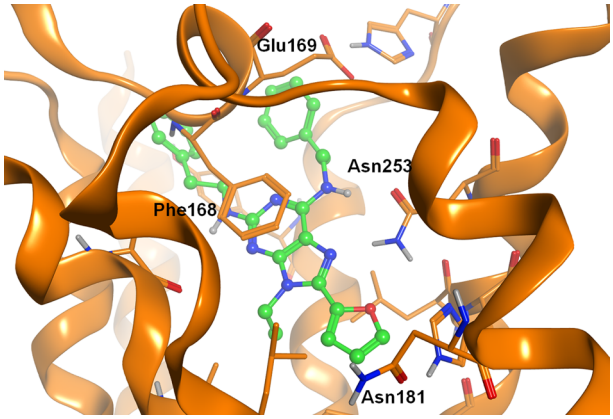

Fig. 6. Docking studies at the $A_{2A}AR$. Docking conformations of compound **17**, with indication of key receptor residues.

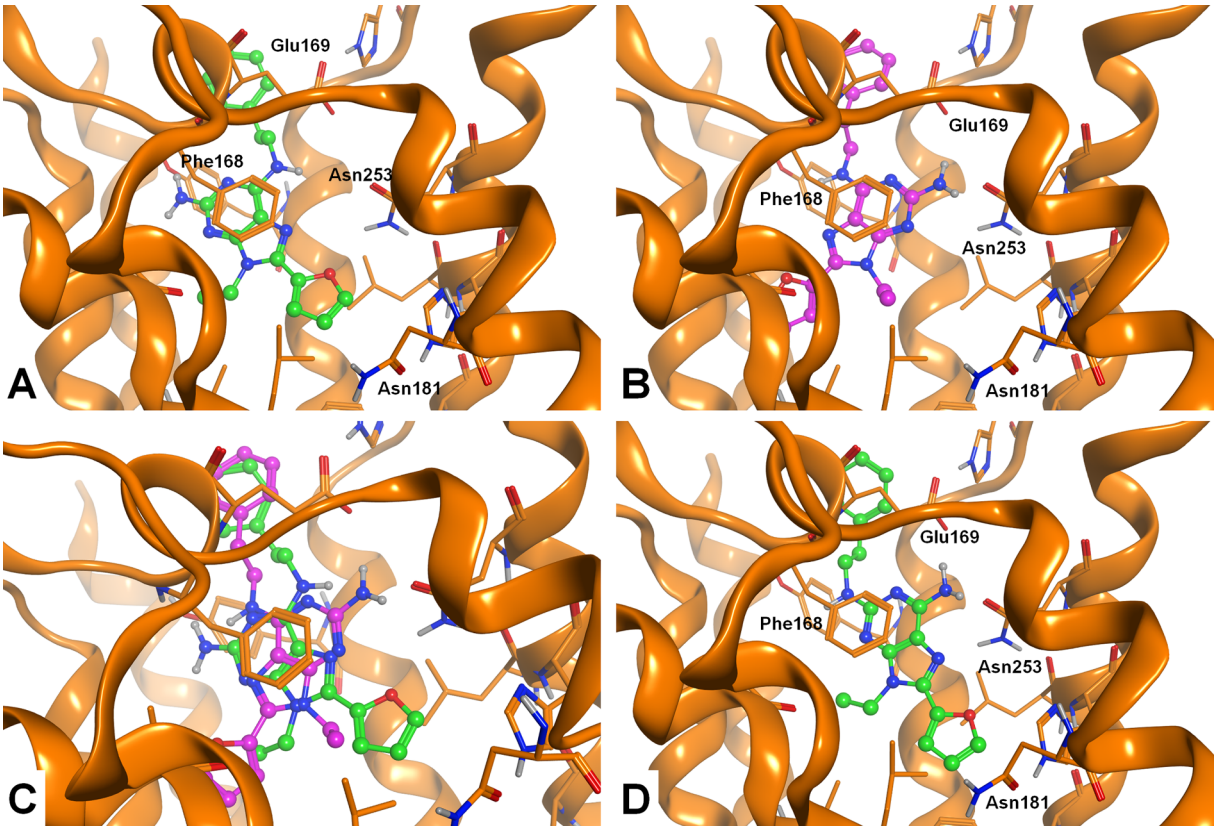

Fig. 5. Docking studies at the $A_{2A}AR$, with key receptor residues indicated. **A and B**. Docking conformations of compound **13**. Binding mode 1 (**A**) and 2 (**B**) are represented. **C**. Superimposition of the two binding modes of compound **13** suggested by docking studies. **D**. Docking conformation of compound **1**.

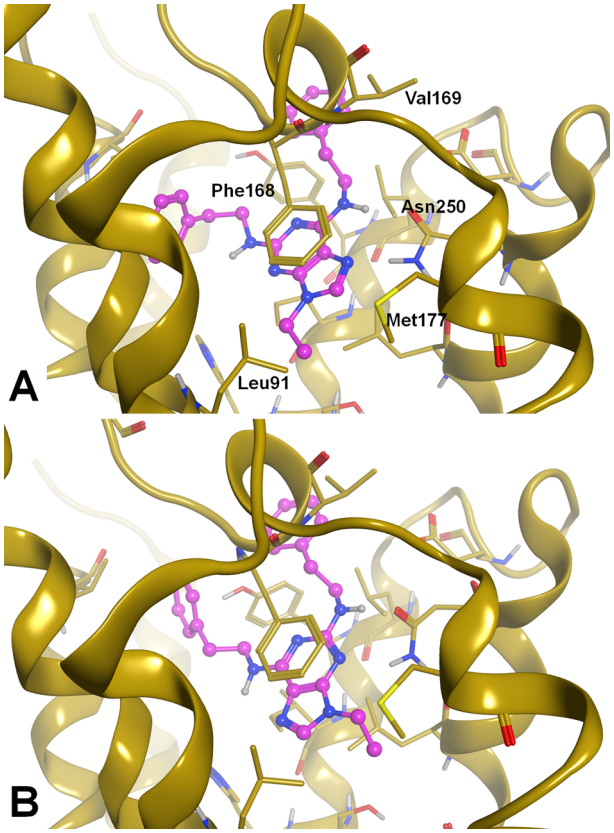

Fig. 7. Docking studies at the A_3AR. Docking conformations of compound **15** as binding mode 1 (**A**) and 2 (**B**) are represented, with indication of key receptor residues.

several A_3AR ligands reported in literature bear arylalkyl groups in a position corresponding to the N^6-substituent of the here reported compound series (i.e. the reference A_3AR agonists IBMECA or 2-Cl-IB-MECA, or other Ado/NECA derivatives [21,44]). Docking studies at a homology model of A_3AR showed that this molecule may adopt both the above described binding modes (Fig. 7A and B). Considering the binding mode 1 arrangement, the N^6-arylalkyl substituent is located in proximity of a hydrophobic valine residue (Val169) that is substituted by a negatively charged glutamate in the other AR subtypes (i.e. Glu169 in the A_{2A}AR [45]). This feature takes to an improved interaction of the A_3AR with the N^6-arylalkyl substituent considering the binding mode 1 arrangement, but also with the 2-arylalkyl substituent considering the binding 2 docking conformations. Docking results at the A_3AR show that favourable docking scores are assigned to both binding modes and hence both binding modes could easily take place within this receptor cavity. The ability of compounds presenting some symmetry to adopt various binding modes within the A_3AR cavity was already observed and reported [46]. Introduction of substituents in the 8-position of **15** led to a significant decrease of A_3AR affinity and selectivity, while the A_{2A}AR affinity resulted generally slightly improved. This may due to different interaction of the compounds with the depth of the A_{2A} and A_3 ARs binding cavity, but also with the effect of the 8-substituent to make the compound able (or not) to adopt various binding modes within the cavities, with consequent higher or lower interaction with the receptor. Among the derivatives of the second set, compounds **15**, **17**, and **19** were tested as A_{2B}AR inhibitors but they did not show any activity at this AR subtype.

Selected derivatives (**V, VI, 1, 7–10, 13**) were tested in CHO cells, stably expressing hA_{2A}AR, in order to assess their ability to inhibit or stimulate the receptor through the evaluation of cAMP production. The results showed that the compounds were not able to stimulate cAMP production (data not shown) and inhibited the NECA-induced increase of cAMP accumulation (see Table 2), behaving as antagonists of the A_{2A}AR. For three of them, **7**, **8**, **10**, endowed with micromolar A_{2A}AR affinity, it was not possible to obtain an IC_{50} value below 50 μM concentration. For the other compounds, the obtained IC_{50} values present an analogue trend of activity compared to the affinity data at the same receptor.

Table 3
Functional activity of compounds **1** and **13** in rat aorta expressed as IC_{50} nM in comparison with the reference agonist CGS 21680 and antagonist ZM 241385. In the table are reported also the K_i data obtained from binding studies at A_{2A}AR subtype.

CPD	EC_{50} [a] (nM)	IC_{50} [b] (nM)	K_i (nM)
CGS 21680	280 *(228–332)*		23 *(18–27)*
ZM 241385		64 *(50–77)*	1.2 *(0.9–1.4)*
1		136 *(93–179)*	3.8 *(3.4–4.2)*
13		589 *(487–690)*	12 *(7.3–16)*

[a] EC_{50} is the concentration of agonists that gives half-maximal response.
[b] IC_{50} is the concentration of antagonists required to produce 50% inhibition of the CGS 21680 relaxation effect. Data are means of 2–4 separated experiments. Values are given as geometric means with 95% confidence intervals in parentheses.

Furthermore, in order to evaluate the efficacy of some new compounds in native tissues, **1** and **13** were tested at rat aorta rings to evaluate their ability to counteract relaxation induced by the selective A_{2A}AR agonist CGS 21680 [47]. The A_{2A}AR antagonist ZM 241385 was also tested for comparison. CGS 21680 showed an EC_{50} = 280 nM whereas ZM 241385 exhibited an IC_{50} = 64 nM. Results confirmed the antagonistic behaviour of the new compounds **1** and **13**, which counteracted the relaxation induced by CGS 21680 with an IC_{50} of 136 nM and 589 nM, respectively (Table 3). These data reveal that **1** and **13** have analogue effect at rat and human A_{2A}ARs demonstrating their usefulness as tools to study pathologies involving the adenosine A_{2A} receptor.

3. Conclusion

Based on the observation that previously reported 9-ethyladenine derivatives bearing arylalkyl groups in the 2-position and an 8-bromo substituent are endowed with nanomolar affinity for the human A_{2A}AR, in this work we further modified these compounds by substituting the 8-bromo atom with a 2-furyl ring, very often associated in literature with high A_{2A}AR affinity. The obtained compounds showed low nanomolar A_{2A}AR K_i data, confirming the hypothesis. From the further observation that 9-ethyladenine derivatives bearing arylalkyl groups in the 2-position or in the N^6-position and an 8-bromo substituent present nanomolar affinity as AR ligands, and following a pharmacophore-based rationale, we developed also a set of 9-ethylpurine derivatives bearing a phenylethylamino- or phenylethyloxy-group in the 6-position and a 2-amine function, to test the effect of these substituents on the affinity at human ARs. Compounds showed low nanomolar affinity in particular for the A_{2A}AR, with the presence of a further 8-substituent modulating the affinity at all the ARs. Docking studies suggested that the substituents inserted in the purine core could make the compounds adopt a sort of upside-down arrangement within the receptor cavity, as compared to the “canonical” binding mode of the reference A_{2A}AR ligand ZM241385. Following these results and observations, we developed a second group of compounds presenting arylalkyl groups at both 2- and 6-positions, to test the effect on AR affinity and subtype selectivity. The second group proved to be slightly A_3AR selective, and again the 8-substituent gave a significant modulation of the AR affinity, with different impact at the various AR subtypes. Docking studies suggested more than one potential binding mode for these compounds, similarly to the first group. These data again suggest the purine core as

a versatile scaffold to develop AR ligands with nanomolar affinity and various degrees of selectivity for the different AR subtypes.

4. Materials and methods

4.1. Chemistry

Melting points were determined with a Büchi apparatus and are uncorrected. ^{1}H NMR spectra were obtained with Varian Gemini 200 or VX 300 MHz spectrometers (^{1}H NMR), (^{13}C NMR); δ values are in ppm, J values are in Hz. All exchangeable protons were confirmed by the addition of D_2O. Mass spectra were recorded on an HP 1100-MSD series instrument. All measurements were performed using electrospray ionization (ESI-MS) on a single quadrupole analyser. Thin-layer chromatography (TLC) was carried out on pre-coated TLC plates with silica gel 60 F_{254} (Fluka). For column chromatography, silica gel 60 (Merck) was used. For preparative TLC, silica gel 20 × 20 cm plates (UV 254 indicator UNIPLATE from Analtech were used. Elemental analyses were determined on Fisons Instruments Model EA 1108 CHNS-O model analyser and are within 0.4% of theoretical values. Purity of the compounds is ≥98% according to elemental analysis data.

4.1.1. General procedure for the synthesis of 8-(furan-2-yl) purine derivatives **1, 2, 12,** and **17**

To the suitable 8-bromo derivatives **V**, **VI**, [33] **11**, or **16** (70 mg, 0.19 mmol), in anhydrous THF (10 mL), 2-(tributylstannyl)furan (in the appropriate amount) and $(PPh_3)_2PdCl_2$ (8 mg, 0.011 mmol) were added and the reaction was left under stirring, in nitrogen atmosphere, at 60 °C, unless otherwise noted, in an oil bath, for the time necessary to the reaction completion. The solvent was removed under vacuum and the crude worked-up as described below.

4.1.1.1. 9-Ethyl-8-(furan-2-yl)–N^2-phenethyl-9H-purine-2,6-diamine (1).

The title compound was obtained by reaction of **V** with 5 equivalents of 2-(tributylstannyl)furan, in 5 h the reaction was complete. The crude residue was purified by preparative thin layer chromatography (TLC) eluting with AcOEt-cC_6H_{12}-CH_3OH (60:37:3). Compound **1** was obtained pure, with 61% yield, after crystallization from CH_3CN. M.p. = 154–156 °C; ^{1}H-NMR (DMSO-d_6, 200 MHz) δ = 1.33 (t, J = 6.7 Hz, 3H, CH_3); 2.87 (t, J = 7.6 Hz, 2H, CH_2-Ph); 3.49 (m, 2H, NH-CH_2); 4.30 (m, 2H, N-CH_2); 6.46 (m, 1H, NH-CH_2); 6.72 (m, 1H, H-Furyl); 6.86 (br s, 2H, NH_2); 6.99 (d, J = 3.6 Hz, 1H, H-Furyl); 7.29 (m, 5H, H-Ph); 7.91 (d, J = 1.4 Hz, 1H, H-Furyl). ESI-MS: positive mode m/z 349.1 $[M+H]^+$, 371.0 $[M+Na]^+$. Elemental analysis calcd for $C_{19}H_{20}N_6O$: C, 65.50; H, 5.79; N, 24.12; found: C, 65.65; H, 5.83; N, 23.91.

4.1.1.2. 9-Ethyl-8-(furan-2-yl)-2-phenethoxy-9H-purin-6-amine (2).

The title compound was obtained by reaction of **VI** with 5 equivalents of 2-(tributylstannyl)furan. The reaction was complete within 3 h. The crude residue was purified by preparative TLC eluting with AcOEt-$CHCl_3$-CH_3OH (65:30:5). Compound **2** was obtained pure, with 39% yield, after crystallization from CH_3OH. M.p. = 173–175 °C; ^{1}H NMR (DMSO-d_6, 200 MHz) δ = 1.33 (t, J = 7.0 Hz, 3H, CH_3); 3.03 (t, J = 7.0 Hz, 2H, CH_2-Ph); 4.35 (q, J = 7.0 Hz, 2H, N-CH_2); 4.45 (t, J = 7.0 Hz, 2H, O-CH_2); 6.74 (m, 1H, H-Furyl); 7.07 (d, J = 3.6 Hz, 1H, H-Furyl); 7.17–7.40 (m, 7H, H-Ph and NH_2); 7.95 (d, 1H, H-Furyl). ESI-MS: positive mode m/z 350.0 $[M+H]^+$, 372.0 $[M+Na]^+$, 699.1 $[2M+H]^+$, 721.1 $[2M+Na]^+$. Elemental analysis calcd for $C_{19}H_{19}N_5O_2$: C, 65.32; H, 5.48; N, 20.04; found: C, 65.39; H, 5.72; N, 19.86.

4.1.1.3. 6-Chloro-9-ethyl-8-(furan-2-yl)-9H-purin-2-amine (12).

The title compound was obtained by reaction of **11** with 2-(tributylstannyl)furan in a 1:1 equivalent ratio. The reaction was complete within 3 h. The crude was purified by normal column chromatography using a dry silica slurry and eluting with $CHCl_3$ – MeCN (99:5). Compound **12** was obtained pure, with 54% yield, after crystallization from $CHCl_3$ – cC_6H_{12}. M.p. = 220–222 °C; ^{1}H NMR = (DMSO-d_6) δ = 1.31 (t, J = 7.2 Hz, 3H, CH_3); 4.34 (m, 2H, N-CH_2); 6.76 (m, 1H, H-Furyl); 7.01 (s, 2H, NH_2); 7.26 (d, J = 3.6 Hz, 1H, H-Furyl); 8.00 (s, 1H, H-Furyl). ESI-MS: positive mode m/z 264.0 $[M+H]^+$, 549.0 $[2M+Na]^+$.

4.1.1.4. 9-Ethyl-8-(furan-2-yl)–N^2,N^6-diphenethyl-9H-purine-2,6-diamine (17).

The title compound was obtained by reaction of **16** with 5 equivalents of 2-(tributylstannyl)furan in an oil bath under reflux for 2.5 h till the reaction was complete. The crude residue was purified by flash column chromatography, dry silica slurry, eluting with nC_6H_{14} – AcOEt (90:10 to 85:15). Compound **17** was obtained as a white solid in 29% yield after crystallization from AcOEt – Et_2O to get. M.p. = 171–173 °C; ^{1}H NMR (DMSO-d_6) δ = 1.32 (m, 3H, NCH_2CH_3), 2.88 (t, J = 6.8 Hz, 2H, CH_2Ph), 2.93 (t, J = 8.0 Hz, 2H, CH_2Ph), 3.56 (m, 2H, N^2CH_2), 3.67 (m, 2H, N^6CH_2), 4.29 (m, 2H, NCH_2CH_3), 6.72 (m, 1H, H-Furyl), 7.03 (m, 1H, H-Furyl), 7.19–7.36 (m, 12H, H-Ph, N^2H, and N^6H), 7.92 (m, 1H, H-Furyl). ESI-MS: positive mode m/z 453.0 $[M+H]^+$, 474.9 $[M+Na]^+$. Elemental analysis calcd for $C_{27}H_{28}N_6O$: C, 71.66; H, 6.24; N, 18.57; found: C, 71.86; H, 6.46; N, 18.34.

4.1.1.5. Synthesis of 6-chloro-9-ethyl-9H-purin-2-amine (4) and 6-chloro-7-ethyl-9H-purin-2-amine (4a).

To a solution of 2-amino-6-chloropurine (**3**, 210 mg, 1.24 mmol) in 6.2 mL of dry DMF K_2CO_3 (215 mg, 1.56 mmol) and 1 equivalent of iodoethane (99 μL; 1.24 mmol) were added. The mixture was left under stirring and under nitrogen atmosphere at r.t. After 5 h the reaction was complete. After evaporation of the solvent, a dry silica slurry was prepared and flash chromatography, eluting with nC_6H_{14} – AcOEt (60:40 to AcOEt 100%), was used to separate the reaction products. Compounds **4** and **4a** were obtained after crystallization from MeCN as pure product with the yield of 66 and 21%, respectively. **4:** m.p. = 154–156 °C; ^{1}H NMR (DMSO-d_6, 400 MHz) δ = 1.35 (t, J = 7.2 Hz, 3H, CH_3); 4.05 (m, 2H, N-CH_2); 6.88 (bs, 2H, NH_2); 8.13 (s, 1H, H-8). **4a:** m.p. = 178 °C (dec.); ^{1}H NMR (DMSO-d_6, 400 MHz) δ = 1.38 (t, J = 7.2 Hz, 3H, CH_3); 4.30 (m, 2H, N-CH_2); 6.62 (br s, 2H, NH_2); 8.37 (s, 1H, H-8).

4.1.2. General procedure for the synthesis of 9-ethyl-N^6-methyl-9H-purine-2,6-diamine (5) and 7-ethyl-N^6-methyl-7H-purine-2,6-diamine (6)

To 2 mL of methylamine, compound **4** or **4a** (100 mg; 0.51 mmol) were in turn added in a steel vial at −80 °C. The vial, well closed, was then brought to r.t. and the reaction was left for 16 h until completion. After evaporation of methylamine at r.t. and coevaporation with MeOH, compound **5** was obtained after crystallization from MeOH in 96% yield; the crude mixture of the reaction of **4a** was chromatographed on silica gel flash column, eluting with $CHCl_3$ – MeOH (93:7–90:10) to get compound **6** in 64% yield.

5: m.p. = 212–214 °C; ^{1}H NMR (DMSO-d_6, 400 MHz) δ = 1.30 (t, J = 7.2 Hz, 3H, CH_3); 2.86 (bs, 3H, N-CH_3); 3.95 (m, 2H, N-CH_2); 5.81 (bs, 2H, NH_2); 7.11 (bs, 1H, NH), 7.67 (s, 1H, H-8). Elemental analysis calcd for $C_8H_{12}N_6$: C, 49.99; H, 6.29; N, 43.72; found: C, 50.32; H, 6.32; N, 43.65.

6: m.p. = 223 °C; ^{1}H NMR (DMSO-d_6, 400 MHz) δ = 1.27 (t, J = 7.2 Hz, 3H, CH_3); 2.88 (d, J = 4.8 Hz, 3H, N-CH_3); 4.26 (q, J = 6.0 Hz, 2H, N-CH_2); 5.55 (bs, 2H, NH_2); 6.45 (m, 1H, NH), 7.84 (s, 1H, H-8).

4.1.2.1. Synthesis of 9-ethyl-N^6-phenethyl-9H-purine-2,6-diamine (7).

Phenethylamine (7 mL) was added to compound **4** (200 mg, 1.01 mmol). The reaction was left under stirring at r.t. for 3.5 h. The phenethylamine was removed under vacuum at high temperature. After preparation of a dry silica slurry, the crude reaction mixture was chromatographed on a flash column, eluting with AcOEt – cC_6H_{12} – MeOH (60:37:3). Compound **7** was obtained after crystallization from

MeCN in 80% yield. M.p. = 106–108 °C; ^{1}H NMR (DMSO-d_6, 400 MHz) δ = 1.31 (t, J = 7.2 Hz, 3H, CH_3); 2.87 (t, J = 7.6 Hz, 2H, CH_2-Ph); 3.59 (br s, 2H, NH-CH_2); 3.96 (q, J = 7.2, 2H, N-CH_2); 5.84 (s, 2H, NH_2); 7.17 (m, 1H, H-Ph); 7.28 (m, 5H, H-Ph and H-8); 7.69 (s, 1H, NH). Elemental analysis calcd for $C_{15}H_{18}N_6$: C, 63.81; H, 6.43; N, 29.77; found: C, 64.05; H, 6.69; N, 29.54.

*4.1.2.2. Synthesis of 9-ethyl-6-phenetoxy-9H-purin-2-amine **(8)***. Phenethyl alcohol (5 mL) was added to compound **4** (200 mg; 1.01 mmol) and, to the solution, 5 equivalents of NaOH (200 mg; 5 mmol) were added and the reaction was left under stirring at r.t. until it was complete after 3.5 h. The solvent was removed by distillation under vacuum; after preparation of a dry slurry, the crude reaction mixture was separated by column chromatography eluting with $CHCl_3$, to elute the phenethyl alcohol in excess, and then with $CHCl_3$-MeOH (99:1) to elute **8**. Compound **8** was obtained after crystallization from MeCN in 57% yield. M.p. = 146–148 °C; ^{1}H NMR (DMSO-d_6, 400 MHz) δ = 1.32 (t, J = 7.4 Hz, 3H, CH_3); 3.06 (t, J = 7.4 Hz, 2H, CH2-Ph); 4.01 (q, J = 7.2 Hz, 2H, N-CH_2); 4.58 (t, J = 7.2 Hz, 2H, O-CH_2); 6.37 (s, 2H, NH_2); 7.31 (m, 5H, H-Ph); 7.58 (s, 1H, H-8). Elemental analysis calcd for $C_{15}H_{17}N_5O$: C, 63.59; H, 6.05; N, 24.72; found: C, 63.86; H, 6.41; N, 24.41.

*4.1.3. General procedure for the preparation of the 8-bromoderivatives **9–11***

To a solution (1 mmol) of the suitable purine derivative **7**, **8**, or **4** in dry DMF (4 mL) the NBS (202 mg; 1.1 mmoles) was added and the reaction mixture was left under stirring and under nitrogen atmosphere at r.t. for the time necessary to the reaction completion. The volatiles were evaporated and a dry silica slurry was prepared with the crude residue and used for the flash chromatography eluted with the suitable solvent.

*4.1.3.1. 8-Bromo-9-ethyl-N^6-phenethyl-9H-purine-2,6-diamine **(9)***. Compound **9** was prepared from compound **7**. The reaction took 10 min for the completion. The crude residue was chromatographed eluting with $CHCl_3$ – MeCN (98:2). Compound **9** was obtained in 80% yield. M.p. = 114–116 °C; ^{1}H NMR (DMSO-d_6, 400 MHz) δ = 1.23 (t, J = 7.0 Hz, 3H, CH_3); 2.85 (t, J = 7.8 Hz, 2H, CH_2-Ph); 3.57 (br s, 2H, NH-CH_2); 3.96 (q, J = 7.0 Hz, 2H, N-CH_2); 6.01 (s, 2H, NH_2); 7.18 (m, 6H, H-Ph and H-8); 7.44 (s, 1H, NH); ESI-MS: positive mode m/z 361.0 $[M+H]^+$, 383.0 $[M+Na]^+$. Elemental analysis calcd for $C_{15}H_{17}BrN_6$: C, 49.87; H, 4.74; N, 23.26; found: C, 50.12; H, 4.98; N, 23.01.

*4.1.3.2. 8-Bromo-9-ethyl-6-phenethoxy-9H-purin-2-amine **(10)***. Compound **10** was prepared from compound **8.** The reaction took 70 min for the completion. The crude residue was chromatographed eluting with *c*C_6H_{12} – AcOEt (60:40) to *c*C_6H_{12} – AcOEt – MeOH (55:40:5). A further purification by preparative TLC was necessary, hence, the obtained impure product was separated with preparative TLC, eluted with AcOEt – *c*C_6H_{12} - MeOH (60:39:1). After crystallization from MeCN, the desired product **10** was obtained in 35% yield. M.p. = 168–171 °C; ^{1}H NMR (DMSO-d_6, 400 MHz) δ = 1.24 (t, J = 7.2 Hz, 3H, CH_3); 3.05 (t, J = 7.2 Hz, 2H, CH_2-Ph); 4.00 (q, J = 7.0 Hz, 2H, N-CH_2); 4.56 (t, J = 7.0 Hz, 2H, O-CH_2); 6.59 (s, 2H, NH_2); 7.21 (m, 1H, H-Ph); 7.31 (m, 4H, H-Ph). ESI-MS: positive mode m/z 362.0 $[M+H]^+$, 384.0 $[M+Na]^+$. Elemental analysis calcd for $C_{15}H_{16}BrN_5O$: C, 49.74; H, 4.45; N, 19.33; found: C, 49.86; H, 4.67; N, 19.14.

*4.1.3.3. 8-Bromo-6-chloro-9-ethyl-9H-purin-2-amine **(11)***. Compound **11** was prepared from compound **4**. The reaction was left for 8 h, then stopped due to the formation of side products. The DMF was removed under vacuum and the crude mixture was partitioned between H_2O and AcOEt. The organic layers were collected, dried over Na_2SO_4, and concentrated to dryness under vacuum. The crude residue was chromatographed eluting with *n*C_6H_{14} – AcOEt (75:25). The collected product was crystallized from CH_2Cl_2 and compound **11** was obtained in 75% yield. M.p. = 182 °C (dec); ^{1}H NMR (DMSO-d_6) δ = 1.27 (t, J = 7.4 Hz, 3H, CH_3); 4.04 (q, J = 7.2 Hz, 2H, N-CH_2); 7.06 (s, 2H, NH_2). ESI-MS: positive mode m/z 276.0 $[M+H]^+$, 297.9 $[M+Na]^+$, 315.9 $[M+K]^+$.

*4.1.3.4. Synthesis of 9-ethyl-8-(furan-2-yl)-N^6-phenethyl-9H-purine-2,6-diamine **(13)***. Compound **12** (75 mg, 0.29 mmol) was added to phenethylamine (3 mL) and left to react under stirring at r.t. until completion after 4 h. The phenethylamine was removed under vacuum and after preparation of a dry silica gel slurry, the crude mixture was chromatographed with a flash column, eluted with $CHCl_3$. Compound **13** was obtained as a pure *vitreous* solid in 90% yield. ^{1}H NMR (DMSO-d_6, 400 MHz) δ = 1.27 (t, J = 7.2 Hz, 3H, CH_3); 2.89 (t, J = 7.6 Hz, 2H, CH_2-Ph); 3.61 (bs, 2H, NH-CH_2); 4.23 (q, J = 7.0 Hz, 2H, N-CH_2); 6.00 (bs, 2H, NH_2); 6.69 (m, 1H, H-Furyl); 6.95 (d, J = 3.6 Hz, 1H, H-Furyl); 7.18 (m, 1H, H-Ph); 7.28 (m, 4H, H-Ph); 7.45 (br s, 1H, NH); 7.87 (s, 1H, H-Furyl). ESI-MS: positive mode m/z 349.1 $[M+H]^+$, 371.1 $[M+Na]^+$. Elemental analysis calcd for $C_{19}H_{20}N_6O$: C, 65.50; H, 5.79; N, 24.12; found: C, 65.77; H, 5.93; N, 23.85.

*4.1.3.5. Synthesis of 9-ethyl-N^2,N^6-diphenethyl-9H-purine-2,6-diamine **(15)***. To 2-phenylethylamine (2 mL) the 2,6-dichloro-9-ethylpurine (**14** [38]; 200 mg; 0.92 mmol) was added in a steel vial and left to react at 120 °C for 16 h. After concentration under vacuum, a dry silica slurry was prepared and purified over a flash column chromatography eluting with CH_2Cl_2 – cC_6H_{12} (75:25 to 100% CH_2Cl_2) to afford **15** as a light yellowish solid after crystallization with CH_3CN. Compound **15** was obtained with 90% yield. M.p. = 102–104 °C; ^{1}H NMR (DMSO-d_6, 400 MHz) δ = 1.34 (t, J = 7.6 Hz, 3H, NCH_2CH_3), 2.85 (t, J = 7.2 Hz, 2H, CH_2Ph), 2.88 (t, J = 8.0 Hz, 2H, CH_2Ph), 3.47 (q, J = 6.4 Hz, 2H, N^2CH_2), 3.63 (br s, 2H, N^6CH_2), 3.99 (q, J = 7.6 Hz, 2H, NCH_2CH$_3$), 6.45 (br s, 1H, N^2H), 7.15–7.27 (m, 11*H*, 2 × Ph and N^6H), 7.70 ppm (s, 1H, H-8). ESI-MS: positive mode m/z 387.1 $[M+H]^+$, 409.0 $[M+Na]^+$. Elemental analysis calcd for $C_{23}H_{26}N_6$: C, 71.47; H, 6.78; N, 21.74; found: C, 71.82; H, 6.91; N, 21.55.

*4.1.3.6. Synthesis of 8-bromo-9-ethyl-N^2,N^6-diphenethyl-9H-purine-2,6-diamine **(16)***. To a mixture of **15** (50 mg; 0.13 mmol), sodium acetate (16 mg; 0.19 mmol), and acetic acid (0.56 mL) bromine (0.4 mL; 0.78 mmol) were added. The mixture was then stirred at r.t. for 12 h, diluted with H_2O (10 mL) and extracted with CH_2Cl_2 (3 × 10 mL). The organic layers were dried over anhydrous Na_2SO_4, filtered, and evaporated to dryness. The crude was purified by flash column chromatography eluting with *c*C_6H_{12}-CH_2Cl_2 (10:90) to CH_2Cl_2/CH_3OH (99.75:0:25) to afford **16** as a yellow powder after crystallization from *c*C_6H_{12} and Et_2O. **16** Was obtained with 85% yield. M.p. = 250 °C (dec); ^{1}H NMR (DMSO-d_6, 400 MHz) δ = 1.25 (t, J = 6.4 Hz, 3H, NCH_2CH_3), 2.85 (m, 3H, CH_2Ph), 2.99 (m, 2H, CH_2Ph), 3.44 (m, 2H, N^2CH_2), 3.60 (br s, 2H, N^6CH_2), 3.98 (q, J = 6.8 Hz, 2H, NCH_2CH$_3$), 6.66 (m, 2H, N^2H & N^6H), 7.13–7.56 (m, 10*H*, H-Ph). ESI-MS: positive mode m/z 465.2 $[M+H]^+$, 467.3 $[M+Na]^+$. Elemental analysis calcd for $C_{23}H_{25}BrN_6$: C, 59.36; H, 5.41; N, 18.06; found: C, 59.61; H, 5.79; N, 17.83.

*4.1.4. General procedure for the preparation of the 8-alkoxypurine derivatives **18** and **19***

Sodium hydroxide (200 mg; 5 mmol) was in turn added to methanol or ethanol (33 mL) at 70 °C and left until dissolution. To the obtained solutions, **16** (70 mg, 0.15 mmol) was added together with another portion of sodium hydroxide (200 mg; 5 mmol) and the reaction mixture was left under stirring, at the same temperature, for the time necessary to the reaction completion. The volatiles were evaporated and a dry silica slurry was prepared with the crude residue and used for the flash chromatography, to be eluted with the suitable solvent.

*4.1.4.1. 9-Ethyl-8-methoxy-N^2,N^6-diphenethyl-9H-purine-2,6-diamine (**18**).* The title compound was obtained by reaction of **16** with methanol for 17 h. Purification by column chromatography eluted with nC_6H_{14} – AcOEt (90:10 to 70:30) gave **18** as vitreous solid with 80% yield. ^{1}H NMR (DMSO-d_6) δ = 1.21 (t, J = 7.2 Hz, 3H, NCH_2CH_3), 2.85 (m, 4H, 2 × CH_2Ph), 3.44 (q, J = 6.4 Hz, 2H, N^2CH_2), 3.62 (br s, 2H, N^6CH_2), 3.81 (q, J = 6.8 Hz, 2H, NCH_2CH_3), 4.00 (s, 3H, OCH_3), 6.29 (br s, 1H, N^2H), 6.87 (br s, 1H, N^6H), 7.17–7.26 ppm (m, 10*H*, H-Ph). ESI-MS: positive mode *m/z* 417.0 $[M+H]^+$, 438.9 $[M+Na]^+$. Elemental analysis calcd for $C_{24}H_{28}N_6O$: C, 69.21; H, 6.78; N, 20.18; found: C, 69.51; H, 6.92; N, 19.99.

*4.1.4.2. 8-Ethoxy-9-ethyl-N^2,N^6-diphenethyl-9H-purine-2,6-diamine (**19**).* The title compound was obtained by reaction of **16** with ethanol for 19 h. Purification by column chromatography eluted with nC_6H_{14} – AcOEt (90:10 to 80:20) gave **19** as vitreous solid with 67% yield. ^{1}H NMR (DMSO-d_6) δ = 1.22 (t, J = 6.8 Hz, 3H, NCH_2CH_3), 1.35 (t, J = 6.8 Hz, 3H, OCH_2CH_3), 2.85 (m, 4H, 2 × CH_2Ph), 3.44 (q, J = 6.0 Hz, 2H, N^2CH_2), 3.62 (br s, 2H, N^6CH_2), 3.80 (q, J = 7.2 Hz, 2H, NCH_2CH_3), 4.41 (q, J = 7.2 Hz, 2H, OCH_2CH_3), 6.27 (br s, 1H, N^2H), 6.82 (br s, 1H, N^6H), 7.15–7.26 ppm (m, 10H, H-Ph). ESI-MS: positive mode *m/z* 431.1 $[M+H]^+$. Elemental analysis calcd for $C_{25}H_{30}N_6O$: C, 69.74; H, 7.02; N, 19.52; found: C, 69.95; H, 7.39; N, 19.31.

*4.1.4.3. Synthesis of 9-ethyl-8-phenethoxy-N^2,N^6-diphenethyl-9H-purine-2,6-diamine (**20**).* To a solution of **16** (70 mg; 0.15 mmol) in dry tetrahydrofuran (2 mL) sodium hydroxide (30 mg; 0.75 mmol) and 2-phenylethanol (120 μL; 1.00 mmol) were added. The reaction was poured at reflux for 72 h. The solvent was removed under vacuum and the crude residue purified by silica gel column, dry silica slurry, eluting with nC_6H_{14} – AcOEt (90:10 to 85:15). The obtained solid was crystallized from nC_6H_{14}-AcOEt and **20** was obtained with 37% yield as off-white powder. M.p. = 250 °C (dec.); ^{1}H NMR (DMSO-d_6) δ = 1.12 (t, J = 6.8 Hz, 3H, NCH_2CH_3), 2.84 (m, 4H, 2 × CH_2Ph), 3.08 (t, J = 6.4 Hz, 2H, OCH_2CH_2Ph), 3.43 (q, J = 6.8 Hz, 2H, N^2CH_2), 3.61 (br s, 2H, N^6CH_2), 3.74 (q, J = 8.0 Hz, 2H, NCH_2CH_3), 4.56 (q, J = 7.2 Hz, 2H, OCH_2), 6.28 (br s, 1H, N^2H), 6.83 (br s, 1H, N^6H), 7.16–7.30 (m, 15H, H-Ph). ESI-MS: positive mode *m/z* 507.1 $[M+H]^+$, 529.0 $[M+Na]^+$. Elemental analysis calcd for $C_{31}H_{34}N_6O$: C, 73.49; H, 6.76; N, 16.59; found: C, 73.68; H, 6.97; N, 16.35.

4.2. Biological evaluation

4.2.1. Cell culture

CHO cells stable transfected with hARs were grown in Dulbecco's modified Eagle's medium (DMEM) with nutrient mixture F12 supplemented with 10% fetal bovine serum (FBS), 100 U/ml penicillin, 100 μg/ml streptomycin, 2.5 μg/ml amphotericin B, 0.1 mg/ml geneticine and 1 mM sodium pyruvate. They were cultured at 37 °C in a humidified atmosphere of 5% CO_2/95% air [38,48].

4.2.2. Membrane preparation

Crude membranes for radioligand binding experiments were prepared by collecting cells (CHO stably transfected with hA_1, hA_{2A} and hA_3 ARs) in ice-cold hypotonic buffer (5 mM Tris/HCl, 2 mM EDTA, pH 7.4). The cell suspension was homogenized on ice (Ultra-Turrax, 2 × 20 s at full speed) and the homogenate was spun for 10 min (4 °C) at 3200 rpm. The supernatant was centrifuged for 50 min at 37,000 rpm at 4 °C. The membrane pellet was resuspended in the specific binding buffer (hA_1AR: 50 mM Tris/HCl buffer, pH 7.4; hA_{2A}AR: 50 mM Tris/HCl, 50 mM $MgCl_2$, pH 7.4; hA_3AR: 50 mM Tris/HCl, 10 mM $MgCl_2$, 1 mM EDTA, pH 8.25), frozen in liquid nitrogen at a protein concentration of 2–4 mg/mL and stored at −80 °C.

4.2.3. Radioligand binding

Dissociation constants of unlabelled compounds (K_i values) were determined in radioligand competition experiments, where a fixed concentration of radioligand (1 nM [^{3}H]CCPA, K_D = 1.1 nM; 10 nM [^{3}H]NECA, K_D = 20 nM; [^{3}H] HEMADO, K_D = 1.5 nM) was incubated in a 96-well plate with 10 μg of specific receptor (hA_1, hA_{2A} and hA_3 ARs, respectively) cell membrane preparations and increasing concentrations of the compound understudy. Non-specific binding was determined in the presence of 1 mM theophylline for hA_1AR and 100 μM (R)-N^6-phenyliso-propyladenosine (R-PIA) for both hA_{2A}AR and hA_3AR. All binding data were calculated by non-linear curve fitting with Prism 5.0 programme (GraphPAD Software, San Diego, CA, USA). Each concentration was tested three-five times in triplicate and the values are given as the mean ± standard errors (S.E.). The activity of the compounds at the hA_{2B}AR was evaluated as inhibition of NECA-stimulated adenylyl cyclase activity.

4.2.4. GloSensor cAMP Assay

Cells, stably expressing the hA_{2A} or hA_{2B} AR and transiently the biosensor, were harvested in CO_2-independent medium and were counted in a Neubauer chamber. The desired number of cells was incubated in equilibration medium containing a 3% v/v GloSensor cAMP reagent stock solution, 10% FBS, and 87% CO_2 independent medium. After 2 h of incubation at rt, the cells were dispensed in the wells of a 384-well plate and, when a steady-state basal signal was obtained, the NECA reference agonist or the understudy compounds, at different concentrations, were added. Initially, the ability of the selected compounds to stimulate the cAMP production was evaluated, but any results were obtained. Subsequently, their antagonist profile was evaluated by assessing their ability to counteract NECA-induced increase of cAMP accumulation. The cells were incubated in the reaction medium (10 min at rt) with different understudy molecule concentrations and then treated with NECA. After 10 min, various luminescence measurements were performed at different incubation times [38,48].

4.2.5. Functional antagonism in isolated rat aorta

All animal testing was carried out according to European Communities Council Directive of 24 November 1986 (86/609/EEC).

Male Wistar rats (275–300 g) were killed by cervical dislocation and the aorta was isolated, freed from adhering connective tissue, and set up rapidly under 1 g resting tension in 10 mL organ baths containing in Krebs solution of the following composition (mM): NaCl, 118.4; KCl, 4.7; $CaCl_2$, 1.9; $MgSO_4$, 1.2; NaH_2PO_4, 1.2; $NaHCO_3$, 25; glucose, 11.7. The preparation was kept at 37 °C and aerated with 5% CO_2: 95% O_2 at pH 7.4 [49]. After at least a 2-hs equilibration period a sub-maximal contractions of aorta rings were obtained by PGF2α (3 μM).

Concentration-response curves were constructed by cumulative addition of the A_{2A} selective agonist CGS 21680 which gives relaxation of the tissue [47]. The concentration of agonist in the organ bath was increased approximately 3-fold at each step, with each addition being made only after the response to the previous addition had attained a minimal level and remained steady. Relaxations were recorded by means of an isometric transducer connected to the MacLab system PowerLab/800. After 30 min the dose-response curve was repeated in the presence of compounds **1**, **13** (used at 1000 nM) or the reference antagonist ZM 241385 (used at 300 nM). In addition, parallel experiments in which tissues did not receive any antagonist were run in order to check any variation in sensitivity.

The IC_{50} values were obtained according to the following equation:

$$K_b = IC_{50}/[1 + (A/EC_{50})^K]$$

in which A = [Ago] = 300 nM, and the K = slope = 0.99.

The K_b values were obtained as follow:

$$K_b = [B]/(DR - 1)$$

where DR is the ratio of EC_{50} values of agonist after and before treatment with antagonist concentration [B].

4.2.6. Statistical analysis

Responses were expressed as percentage of the maximal relative luminescence units (RLU). Concentration–response curves were fitted by a nonlinear regression with the Prism 5.0 programme (GraphPAD Software, San Diego, CA, USA). The antagonist profile of the two compounds was expressed as IC_{50}. The IC_{50} value is the concentration of antagonists that produces 50% inhibition of the agonist effect. Each concentration was tested three-five times in triplicate and the values are given as geometric means with 95% confidence intervals in parentheses [50].

4.3. Molecular modeling

A high-resolution crystal structures of the $hA_{2A}AR$ in complex with ZM241385 was retrieved from the Protein Data Bank (http://www.rcsb.org; pdb code: 5NM4; 1.7-Å resolution [41]). The structure was modified by rebuilding the missing IL3 segment and by mutating some residues to restore the wild type sequence. The Homology Modeling tool of MOE [51] was used for this task. Hydrogen atoms were added and energetically minimized. A homology model of the human A_3AR was built following a procedure previously reported [43]. The Homology Modeling tool of MOE was employed even for this task. All compound structures were docked into the binding site of the hA_{2A} and hA_3 ARs structure using the genetic algorithm docking tool of CCDC Gold [42] with default efficiency settings and by selecting GoldScore as scoring function [42].

Declaration of Competing Interest

The authors declare no conflict of interest.

Acknowledgements

This work was supported by the University of Camerino (Progetto FAR FPI000042) and by a grant from the Ministry of Research (PRIN N° 2015E8EMCM_008, 2015).

References

[1] B.B. Fredholm, A.P. IJzerman, K.A. Jacobson, K.-N. Klotz, J. Linden, International Union of Pharmacology. XXV. Nomenclature and classification of adenosine receptors, Pharmacol. Rev. 53 (2001) 527–552.
[2] B.B. Fredholm, A.P. IJzerman, K.A. Jacobson, J. Linden, C.E. Muller, International Union of Basic and Clinical Pharmacology. LXXXI. Nomenclature and Classification of Adenosine Receptors–An Update, Pharmacol. Rev. 63 (1) (2011) 1–34, https://doi.org/10.1124/pr.110.003285.
[3] T.W. Hein, W. Wang, B. Zoghi, M. Muthuchamy, L. Kuo, Functional and molecular characterization of receptor subtypes mediating coronary microvascular dilation to adenosine, J. Mol. Cell. Cardiol. 33 (2001) 271–282, https://doi.org/10.1006/jmcc.2000.1298.
[4] Z. Zhou, U. Rajamani, H. Labazi, S.L. Tilley, C. Ledent, B. Teng, S.J. Mustafa, Involvement of NADPH oxidase in A_{2A} adenosine receptor-mediated increase in coronary flow in isolated mouse hearts, Purinergic Signal. 11 (2015) 263–273, https://doi.org/10.1007/s11302-015-9451-x.
[5] J.P. Headrick, K.J. Ashton, R.B. Rose'meyer, J.N. Peart, Cardiovascular adenosine receptors: expression, actions and interactions, Pharmacol. Ther. 140 (2013) 92–111, https://doi.org/10.1016/j.pharmthera.2013.06.002.
[6] L. Antonioli, C. Blandizzi, P. Pacher, G. Hasko, Immunity, inflammation and cancer: a leading role for adenosine, Nat. Rev. Cancer 13 (2013) 842–857, https://doi.org/10.1038/nrc3613.
[7] N. Dale, A.M. Sebastiao, Dissecting neurovascular coupling mechanisms: a role for adenosine A_{2A} receptor: an Editorial highlight for 'Correlation of transient adenosine release and oxygen changes in the caudate-putamen', J. Neurochem. 140 (2017) 10–12, https://doi.org/10.1111/jnc.13896.
[8] D. Dal Ben, L. Antonioli, C. Lambertucci, M. Fornai, C. Blandizzi, R. Volpini, Purinergic ligands as potential therapeutic tools for the treatment of inflammation-related intestinal diseases, Front. Pharmacol. 9 (2018) 212, https://doi.org/10.3389/fphar.2018.00212.
[9] T. Porkka-Heiskanen, A.V. Kalinchuk, Adenosine, energy metabolism and sleep homeostasis, Sleep Med. Rev. 15 (2011) 123–135, https://doi.org/10.1016/j.smrv.2010.06.005.
[10] R. Basheer, R.E. Strecker, M.M. Thakkar, R.W. McCarley, Adenosine and sleep-wake regulation, Prog. Neurobiol. 73 (2004) 379–396, https://doi.org/10.1016/j.pneurobio.2004.06.004.
[11] R.N. Takahashi, F.A. Pamplona, R.D. Prediger, Adenosine receptor antagonists for cognitive dysfunction: a review of animal studies, Front. Biosci. 13 (2008) 2614–2632, https://doi.org/10.2741/2870.
[12] C.N. Wilson, S.J. Mustafa, Adenosine receptors in health and disease, Handb. Exp. Pharmacol. vol. 193, Springer, Berlin, Heidelberg, 2009, , https://doi.org/10.1007/978-3-540-89615-9.
[13] D. Boison, Adenosine dysfunction and adenosine kinase in epileptogenesis, Open Neurosci. J. 4 (2010) 93–101, https://doi.org/10.2174/1874082001004020093.
[14] P. Popoli, R. Pepponi, Potential therapeutic relevance of adenosine A_{2B} and A_{2A} receptors in the central nervous system, CNS Neurol. Disord. Drug Targets 11 (2012) 664–674, https://doi.org/10.2174/187152712803581100.
[15] D. Boison, U.S. Sandau, D.N. Ruskin, M. Kawamura Jr., S.A. Masino, Homeostatic control of brain function - new approaches to understand epileptogenesis, Front. Cell. Neurosci. 7 (2013) 109, https://doi.org/10.3389/fncel.2013.00109.
[16] S. Kashfi, K. Ghaedi, H. Baharvand, M.H. Nasr-Esfahani, M. Javan, A_1 adenosine receptor activation modulates central nervous system development and repair, Mol. Neurobiol. 54 (2017) 8128–8139, https://doi.org/10.1007/s12035-016-0292-6.
[17] K. Varani, F. Vincenzi, S. Merighi, S. Gessi, P.A. Borea, Biochemical and pharmacological role of A_1 adenosine receptors and their modulation as novel therapeutic strategy, Adv. Exp. Med. Biol. (2017), https://doi.org/10.1007/5584_2017_61.
[18] M. de Lera Ruiz, Y.H. Lim, J. Zheng, Adenosine A_{2A} receptor as a drug discovery target, J. Med. Chem. 57 (2014) 3623–3650, https://doi.org/10.1021/jm4011669.
[19] A. van Waarde, R. Dierckx, X. Zhou, S. Khanapur, H. Tsukada, K. Ishiwata, G. Luurtsema, E.F.J. de Vries, P.H. Elsinga, Potential therapeutic applications of adenosine A_{2A} receptor ligands and opportunities for A_{2A} receptor imaging, Med. Res. Rev. 38 (2018) 5–56, https://doi.org/10.1002/med.21432.
[20] C.M. Aherne, E.M. Kewley, H.K. Eltzschig, The resurgence of A_{2B} adenosine receptor signaling, Biochim. Biophys. Acta 2011 (1808) 1329–1339, https://doi.org/10.1016/j.bbamem.2010.05.016.
[21] S.L. Cheong, S. Federico, G. Venkatesan, A.L. Mandel, Y.M. Shao, S. Moro, G. Spalluto, G. Pastorin, The A_3 adenosine receptor as multifaceted therapeutic target: pharmacology, medicinal chemistry, and in silico approaches, Med. Res. Rev. 33 (2013) 235–335, https://doi.org/10.1002/med.20254.
[22] CVT, CV Therapeutics and Astellas Announce FDA Approval for Lexiscan(TM) (regadenoson) Injection http://www.cvt.com/PressRelease.aspx?releaseID=1128317, 2008.
[23] L. Lopez-Cruz, J.D. Salamone, M. Correa, Caffeine and selective adenosine receptor antagonists as new therapeutic tools for the motivational symptoms of depression, Front. Pharmacol. 9 (2018) 526, https://doi.org/10.3389/fphar.2018.00526.
[24] L. Gallelli, D. Falcone, R. Cannataro, M. Perri, R. Serra, G. Pelaia, R. Maselli, R. Savino, G. Spaziano, B. D'Agostino, Theophylline action on primary human bronchial epithelial cells under proinflammatory stimuli and steroidal drugs: a therapeutic rationale approach, Drug Des. Devel. Ther. 11 (2017) 265–272, https://doi.org/10.2147/DDDT.S118485.
[25] R. Dungo, E.D. Deeks, Istradefylline: first global approval, Drugs 73 (2013) 875–882, https://doi.org/10.1007/s40265-013-0066-7.
[26] C.E. Muller, K.A. Jacobson, Xanthines as adenosine receptor antagonists, Handb. Exp. Pharmacol. (2011) 151–199, https://doi.org/10.1007/978-3-642-13443-2_6.
[27] W.F. Kiesman, E. Elzein, J. Zablocki, A_1 adenosine receptor antagonists, agonists, and allosteric enhancers, Handb. Exp. Pharmacol. (2009) 25–58, https://doi.org/10.1007/978-3-540-89615-9_2.
[28] B. Cacciari, G. Spalluto, S. Federico, A_{2A} adenosine receptor antagonists as therapeutic candidates: are they still an interesting challenge? Mini Rev. Med. Chem. 18 (2018) 1168–1174, https://doi.org/10.2174/1389557518666180423113051.
[29] R.V. Kalla, J. Zablocki, Progress in the discovery of selective, high affinity A_{2B} adenosine receptor antagonists as clinical candidates, Purinergic Signal. 5 (2009) 21–29, https://doi.org/10.1007/s11302-008-9119-x.
[30] P.A. Borea, K. Varani, F. Vincenzi, P.G. Baraldi, M.A. Tabrizi, S. Merighi, S. Gessi, The A_3 adenosine receptor: history and perspectives, Pharmacol. Rev. 67 (2015) 74–102, https://doi.org/10.1124/pr.113.008540.
[31] E. Camaioni, S. Costanzi, S. Vittori, R. Volpini, K.-N. Klotz, G. Cristalli, New substituted 9-alkylpurines as adenosine receptor ligands, Bioorg. Med. Chem. 6 (1998) 523–533, https://doi.org/10.1016/S0968-0896(98)00007-8.
[32] K.-N. Klotz, S. Kachler, C. Lambertucci, S. Vittori, R. Volpini, G. Cristalli, 9-Ethyladenine derivatives as adenosine receptor antagonists: 2- and 8-substitution results in distinct selectivities, Naunyn-Schmiedeberg's Arch. Pharmacol. 367 (2003) 629–634, https://doi.org/10.1007/s00210-003-0749-9.
[33] C. Lambertucci, S. Vittori, R.C. Mishra, D. Dal Ben, K.-N. Klotz, R. Volpini, G. Cristalli, Synthesis and biological activity of trisubstituted adenines as A_{2A} adenosine receptor antagonists, Nucleosides Nucleotides Nucleic Acids 26 (2007) 1443–1446, https://doi.org/10.1080/15257770701542264.
[34] C. Lambertucci, G. Cristalli, D. Dal Ben, D.D. Kachare, C. Bolcato, K.-N. Klotz, G. Spalluto, R. Volpini, New 2,6,9-trisubstituted adenines as adenosine receptor antagonists: a preliminary SAR profile, Purinergic Signal. 3 (2007) 339–346, https://doi.org/10.1007/s11302-007-9068-9.
[35] C. Lambertucci, I. Antonini, M. Buccioni, D. Dal Ben, D.D. Kachare, R. Volpini, K.-N. Klotz, G. Cristalli, 8-Bromo-9-alkyl adenine derivatives as tools for developing new adenosine A_{2A} and A_{2B} receptors ligands, Bioorg. Med. Chem. 17 (2009) 2812–2822, https://doi.org/10.1016/j.bmc.2009.02.030.
[36] D. Dal Ben, M. Buccioni, C. Lambertucci, A. Thomas, K.-N. Klotz, S. Federico, B. Cacciari, G. Spalluto, R. Volpini, 8-(2-Furyl)adenine derivatives as A_{2A} adenosine receptor ligands, Eur. J. Med. Chem. 70C (2013) 525–535, https://doi.org/10.1016/j.ejmech.2013.10.006.
[37] C. Lambertucci, G. Marucci, D. Dal Ben, M. Buccioni, A. Spinaci, S. Kachler, K.-N. Klotz, R. Volpini, New potent and selective A_1 adenosine receptor antagonists as potential tools for the treatment of gastrointestinal diseases, Eur. J. Med. Chem. 151

(2018) 199–213, https://doi.org/10.1016/j.ejmech.2018.03.067.
[38] A. Thomas, M. Buccioni, D. Dal Ben, C. Lambertucci, G. Marucci, C. Santinelli, A. Spinaci, S. Kachler, K.-N. Klotz, R. Volpini, The length and flexibility of the 2-substituent of 9-ethyladenine derivatives modulate affinity and selectivity for the human A_{2A} adenosine receptor, ChemMedChem 11 (2016) 1829–1839, https://doi.org/10.1002/cmdc.201500595.
[39] R. Volpini, D. Dal Ben, C. Lambertucci, G. Marucci, R.C. Mishra, A.T. Ramadori, K.-N. Klotz, M.L. Trincavelli, C. Martini, G. Cristalli, Adenosine A_{2A} receptor antagonists: new 8-substituted 9-ethyladenines as tools for in vivo rat models of Parkinson's disease, ChemMedChem 4 (2009) 1010–1019, https://doi.org/10.1002/cmdc.200800434.
[40] C. Lambertucci, M. Buccioni, D. Dal Ben, S. Kachler, G. Marucci, A. Spinaci, A. Thomas, K.-N. Klotz, R. Volpini, New substituted 9-propyladenine derivatives as A_{2A} adenosine receptor antagonists, MedChemComm 6 (2015) 963–970, https://doi.org/10.1039/c5md00034c.
[41] T. Weinert, N. Olieric, R. Cheng, S. Brunle, D. James, D. Ozerov, D. Gashi, L. Vera, M. Marsh, K. Jaeger, F. Dworkowski, E. Panepucci, S. Basu, P. Skopintsev, A.S. Dore, T. Geng, R.M. Cooke, M. Liang, A.E. Prota, V. Panneels, P. Nogly, U. Ermler, G. Schertler, M. Hennig, M.O. Steinmetz, M. Wang, J. Standfuss, Serial millisecond crystallography for routine room-temperature structure determination at synchrotrons, Nat. Commun. 8 (2017) 542, https://doi.org/10.1038/s41467-017-00630-4.
[42] G. Jones, P. Willett, R.C. Glen, A.R. Leach, R. Taylor, Development and validation of a genetic algorithm for flexible docking, J. Mol. Biol. 267 (1997) 727–748, https://doi.org/10.1006/jmbi.1996.0897.
[43] M. Falsini, L. Squarcialupi, D. Catarzi, F. Varano, M. Betti, D. Dal Ben, G. Marucci, M. Buccioni, R. Volpini, T. De Vita, A. Cavalli, V. Colotta, The 1,2,4-triazolo[4,3-a]pyrazin-3-one as a versatile scaffold for the design of potent adenosine human receptor antagonists. Structural investigations to target the A_{2A} receptor subtype, J. Med. Chem. 60 (2017) 5772–5790, https://doi.org/10.1021/acs.jmedchem.7b00457.
[44] P.G. Baraldi, B. Cacciari, M.J. Pineda de Las Infantas, R. Romagnoli, G. Spalluto, R. Volpini, S. Costanzi, S. Vittori, G. Cristalli, N. Melman, K.S. Park, X.D. Ji, K.A. Jacobson, Synthesis and biological activity of a new series of N^6-arylcarbamoyl, 2-(Ar)alkynyl-N^6-arylcarbamoyl, and N^6-carboxamido derivatives of adenosine-5'-*N*-ethyluronamide as A_1 and A_3 adenosine receptor agonists, J. Med. Chem. 41 (1998) 3171–3185, https://doi.org/10.1021/jm980147p.
[45] D. Dal Ben, C. Lambertucci, G. Marucci, R. Volpini, G. Cristalli, Adenosine receptor modeling: what does the A_{2A} crystal structure tell us? Curr. Top. Med. Chem. 10 (2010) 993–1018, https://doi.org/10.2174/156802610791293145.
[46] V. Colotta, F. Capelli, O. Lenzi, D. Catarzi, F. Varano, D. Poli, F. Vincenzi, K. Varani, P.A. Borea, D. Dal Ben, R. Volpini, G. Cristalli, G. Filacchioni, Novel potent and highly selective human A_3 adenosine receptor antagonists belonging to the 4-amido-2-arylpyrazolo[3,4-c]quinoline series: molecular docking analysis and pharmacological studies, Bioorg. Med. Chem. 17 (2009) 401–410, https://doi.org/10.1016/j.bmc.2008.10.018.
[47] A. Monopoli, A. Conti, C. Zocchi, C. Casati, R. Volpini, G. Cristalli, E. Ongini, Pharmacology of the new selective A_{2A} adenosine receptor agonist 2-hexynyl-5'-*N*-ethylcarboxamidoadenosine, Arzneimittelforschung 44 (1994) 1296–1304.
[48] M. Buccioni, C. Santinelli, P. Angeli, D. Dal Ben, C. Lambertucci, A. Thomas, R. Volpini, G. Marucci, Overview on radiolabel-free in vitro assays for GPCRs, Mini Rev. Med. Chem. 17 (2017) 3–14, https://doi.org/10.2174/1389557516666160808120207.
[49] G. Sagratini, M. Buccioni, G. Marucci, E. Poggesi, M. Skorski, S. Costanzi, D. Giardina, Chiral analogues of (+)-cyclazosin as potent alpha1B-adrenoceptor selective antagonist, Bioorg Med Chem 26 (2018) 3502–3513, https://doi.org/10.1016/j.bmc.2018.05.023.
[50] M. Buccioni, G. Marucci, D. Dal Ben, D. Giacobbe, C. Lambertucci, L. Soverchia, A. Thomas, R. Volpini, G. Cristalli, Innovative functional cAMP assay for studying G protein-coupled receptors: application to the pharmacological characterization of GPR17, Purinergic Signal. 7 (2011) 463–468, https://doi.org/10.1007/s11302-011-9245-8.
[51] Molecular Operating Environment; C.C.G., 1255 University St., Suite 1600, Montreal, Quebec, Canada, H3B 3X3.